Journal of Applied Geophysics 175 (2020) 103970

Contents lists available at ScienceDirect

Journal of Applied Geophysics

journal homepage: www.elsevier.com/locate/jappgeo

Causes and effects of the AIP trap in AEM data

Andrea Viezzoli [a,*], Giovanni Manca [b], Chris Wjins [c]

[a] Aarhus Geophysics Aps, Risskov, Denmark
[b] Aarhus Geofisica srl, Pisa, Italy
[c] First Quantum Minerals Ltd, Perth, Australia

ARTICLE INFO

Article history:
Received 28 February 2019
Received in revised form 8 February 2020
Accepted 9 February 2020
Available online 10 February 2020

Keywords:
AIP
IP
AEM
Near-surface
SkyTEM
12.5 Hz

ABSTRACT

In the presence of shallow chargeable layers and resistive basement, IP effects in AEM data can severely alter the relationship between depth and voltage measured in the receiver at a given time. The contribution of the IP currents from the shallow layers can overcome that of the downward moving EM currents. As a result, the contribution of the total currents to the entire recorded transient may effectively remain trapped in the near-surface chargeable layer, with a phenomenon we call the “AIP trap”. The AEM data therefore become more sensitive to the near-surface geology. They also become more sensitive to AEM systems' altitude variations. These effects can be especially relevant for AEM systems with slow ramps, which otherwise display limited near-surface resolution. The implication is a larger range of possible applications of AEM systems to mapping of, e.g., bedrock topography, permafrost, clays in regolith, and other layers relevant to geotechnics, where these layers demonstrate some chargeability. SkyTEM 12.5 Hz data from southern Spain are particularly affected by IP in areas of conductive cover. By reducing artefacts in the resistivity models derived from inversion, modelling IP improves the prediction of depth to resistive basement within a certain range of cover thickness.

1. Introduction

IP effects are often present to some extent in AEM data. Sometimes referred to as airborne IP (AIP), these effects are not always visually recognisable in EM decay curves. They have been ignored for decades in the history of EM modelling, including inversion. Recent research effort has concentrated on extracting the IP signal from airborne EM to both improve the recovered conductivity values and present the IP as a separate dataset (e.g., Macnae, 2016a and b; Viezzoli et al., 2017; Kang et al., 2017; Viezzoli and Manca, 2019). However, the existing bibliography does not highlight the fact that the presence of chargeable material can significantly alter the relationship between measured voltage versus time and depth, which forms the basis for EM inversion, and from which the correlation between conductance and sensitivity derives. We demonstrate the implications of this altered relationship, where, even at late times, a major part of the signal at the receiver may originate in shallow, chargeable ground. This phenomenon, which we have named the “AIP trap”, is not fully investigated and openly addressed in the literature, despite its fundamental relevance to the application of AEM. Modelling and inversion of AEM data is compromised by ignoring AIP, to the point of misleading interpretation of results. By describing the basic effects and the physical situations in which they occur, we alert processors and interpreters of EM data to possible pitfalls and the need to mitigate the consequences of the phenomenon.

2. Method and results

One of the bases of the standard TDEM (pure induction) theory for a concentric loop set up over a layered earth is the monotonically increasing relationship between depth of investigation and time (e.g., Nabighian, 1979). In the presence of chargeability in the subsurface, this general relationship ceases to be valid. The electrically dispersive material $\rho(\omega)$, where ρ = resistivity, ω = frequency, once charged up, discharges over a period of time (producing the IP current). Until the discharge is complete, it provides an added contribution to the total induced currents ($\mathbf{J}_{tot}$). Under the quasi static assumption, the latter becomes the sum of pure induction ($\mathbf{J}_{em}$) and IP ($\mathbf{J}_{ip}$) currents, which have opposite directions. This scenario is well known and has been well described decades ago by, e.g., Smith (1989). What has not been fully addressed and recognized is one specific implication: as a consequence of the duration of IP currents, a significant portion of the voltage measured at the receiver may, as time progresses, not come from deeper ground. Under the right circumstances, the measured signal can originate, for the entire transient, from a shallow chargeable layer of moderate conductivity. This process is illustrated in Fig. 1, for a shallow chargeable layer (e.g., permafrost or clay in weathered regolith) over resistive basement (e.g., fresh rock). The response is that of a

* Corresponding author.
E-mail addresses: av@aarhusgeo.com (A. Viezzoli), gm@aarhusgeo.com (G. Manca), chris.wijns@fqml.com (C. Wjins).

https://doi.org/10.1016/j.jappgeo.2020.103970
0926-9851/

nominal 25 Hz, concentric loop, time domain AEM system, with ground clearance of 30 m, and a trapezoidal waveform with ~1 ms ramp down duration. Refer to Viezzoli et al. (2017) for full details on the modelling.

The top panels qualitatively represent the paths of the EM and IP currents. In order to more easily follow the correlation between currents and measured transient, the middle panels illustrate the transient for the magnetic field B, which is linearly dependent on the sum of the currents (EM plus IP), and the lower panels demonstrate the more common time derivative of the magnetic field dB/dt (dependent on the time derivative of the sum of the currents). The total contribution to B($\mathbf{J}_{tot}$) is given by the sum of B($\mathbf{J}_{em}$) and B($\mathbf{J}_{ip}$), and the same is true for dB/dt. B ($\mathbf{J}_{ip}$) is calculated subtracting B($\mathbf{J}_{em}$) from B($\mathbf{J}_{tot}$). The model is based on a simple two-layer scenario, where the first layer is chargeable. At very early times, the induced EM field enters the first layer, where the chargeable (dispersive) material responds by creating a current with both a pure EM ($\mathbf{J}_{em}$) and an IP component ($\mathbf{J}_{ip}$). From that moment onward, the two currents separate vertically. The EM currents continue diffusing downward to a depth that can be approximated by the diffusion depth Z(t,ρ) = sqrt(2tρ/μ0) (where t = time, μ0 = magnetic permeability of free space), then enter the non-dispersive, more resistive second layer. The IP current, on the other hand, does not travel deeper than the bottom of the chargeable first layer, and its rate of decay depends on the specific time constant τof this layer. At a certain time and for a strong enough chargeability, the B field measured by the receiver at surface is effectively due to $\mathbf{J}_{ip}$ only. We call this stage of the transient the "AIP trap". This focusing of the measured signal in the near surface implies a change in the sensitivity of the AEM system to different depths. The near surface should see an increase in sensitivity.

Synthetic modelling of a variety of 1D layered earth scenarios demonstrates the AIP trap and its effect on near surface sensitivity. We calculate forward responses (with added random noise of 5%) and associated sensitivities of nominal AEM systems using the modelling code AarhusInv, replacing the standard non-dispersive resistivity by the Cole-Cole model of Eq. (1) (cf Fiandaca et al., 2012).

$$\zeta(\omega) = \rho\left[1-\frac{m}{10^3}\left(1-\frac{1}{1+(i\omega\tau)^C}\right)\right] \tag{1}$$

There are four interconnected parameters in this equation yielding the complex, dispersive impedance $\zeta(\omega)$: the electrical resistivity ρ (ohm m), the chargeability m (mV/V), the relaxation constant τ (s),

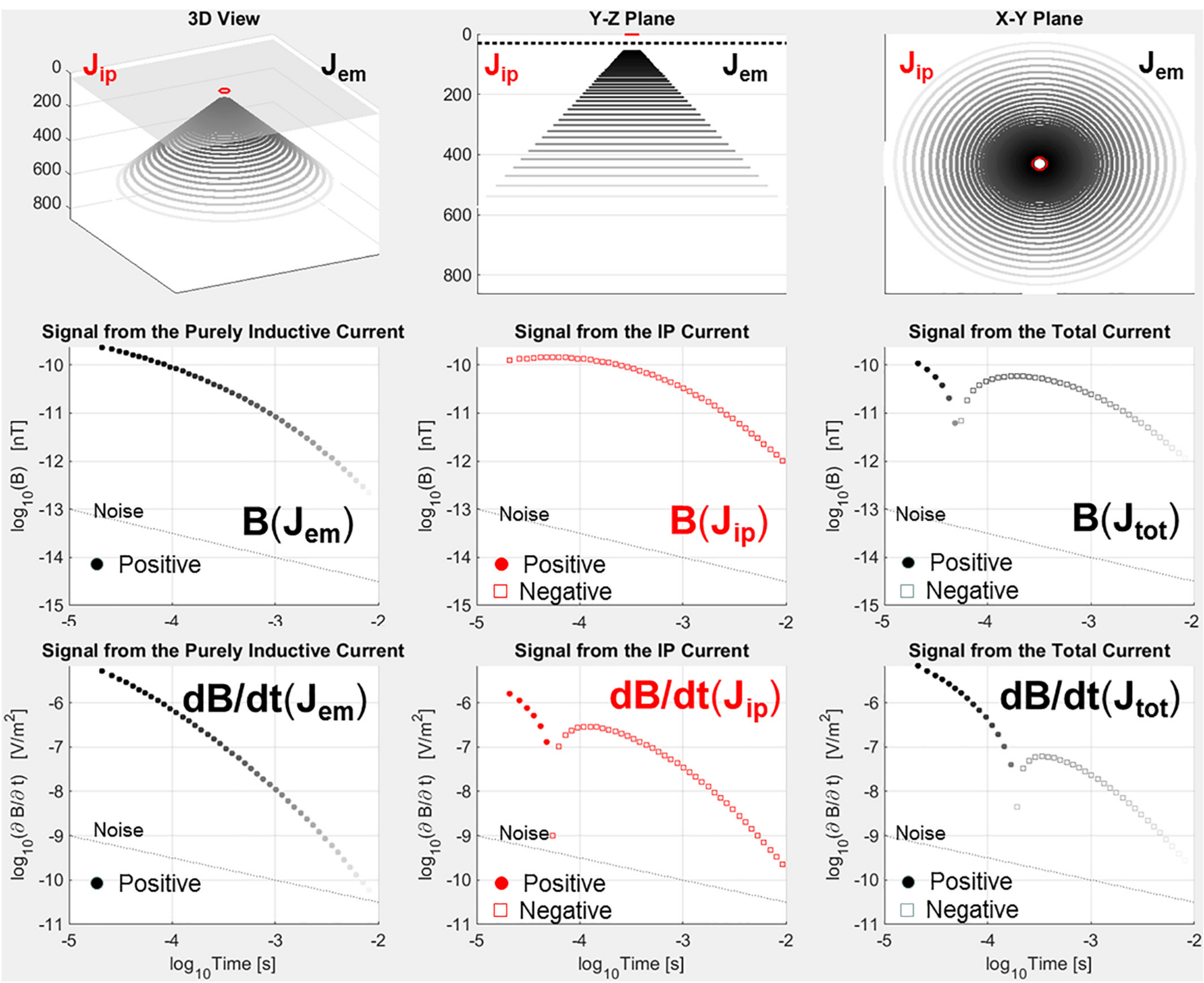

Fig. 1. (Top panels) Qualitative paths of EM (grey rings) and IP (red ring) currents (layered earth, 1D), versus their relative contributions in measured responses for B (middle panels) and dB/dt (bottom panels), in the presence of a shallow chargeable layer (30 m, ρ = 100 Ωm, m = 300 mV/V, c = 0.5, $t = 10^{-3}$ s), above a resistive (ρ = 1000 Ωm) and non-chargeable bedrock. Full symbols represent positive readings, empy symbols negatives.

and the frequency parameter c. A frequency dependent term is also added to the pure EM conductance. Our modelling results simulate a helicopter-borne central loop system, with specifications similar to a modern "VTEM Max" system (Geotech Ltd) with a 25 Hz base frequency and the first time gate centred at ~20 μs from the end of the current turn-off ramp (approximately 1 ms long). We first compare the variations of forward responses as a function of the thickness of the first shallow layer, with and without chargeability. Fig. 2 shows how the presence of chargeable material in a thin layer over a resistive half-space dramatically increases the sensitivity of the AEM system to the thickness of the first layer. The VTEM forward responses associated with small increments of thickness of the top chargeable layer from 2 m to 10 m vary by approximately an order of magnitude. When the top layer is non-chargeable, the variation is only a few percent.

Forward responses over a suite of models produce more generalised and quantitative results. The models contain two layers, with a fixed, resistive, non-chargeable bottom layer and a 20 m thick top layer of varying resistivity and chargeability. We calculate 10,000 responses associated with all possible combinations of Cole-Cole parameters for the top layer (Table 1), varied in discrete steps within given ranges.

We then calculate the sensitivity for all parameters, including the thickness of the top layer, from the linearized approximation of the covariance matrix (e.g., Auken and Christiansen, 2004), which takes expected noise levels into account. The analysis gives a standard deviation factor (STDF) for every parameter (of value = q) which provides the boundaries of one standard deviation (68%) likelihood of a parameter variance (between q/STDFq and q*STDFq). Therefore, STDF = 1 represents no model uncertainty (not possible) and larger numbers mean an increase in uncertainty (e.g., 1.1 is 10% and 2 is 100% uncertainty).

Fig. 3a is a 3D view of the sensitivity (expressed as Log10(STDF-1)) of the *thickness* of the first layer versus resistivity, chargeability, and Cole-Cole constant c for a constant τ value of 10^{-4} s. Warm colours indicate better sensitivities, and therefore lower uncertainty on model parameter. Fig. 3b displays the sensitivity of the *resistivity* of the top layer and Fig. 3c shows the sensitivity of the *chargeability* of the top layer. There is a domain of this 4D hyperspace where sensitivity to the parameters ρ, thickness, and *m* of the first layer improve (lower uncertainty) significantly when its chargeability m and conductivity increase. This confirms the heightened near-surface sensitivity expected from the above description of the physics of the phenomenon, and the results of Figs. 2 and 3.

Table 1
Summary of the values of the Cole-Cole parameters used, in all their possible combinations, for the calculation of the forward responses.

	ρ (Ωm)	m (mV/V)	c	τ (s)
N steps	10	10	10	10
Minimum value	1	0	0.1	10^{-6}
Maximum value	10^4	900	1	$5*10^{-2}$
Increment	~1/3 decade	100	0.1	1/2 decade

Sensitivity to the top layer (not shown) displays a more complex relationship with τ where sensitivity gradients of different signs depend on a range of τ gradients).This is a consequence of the limited frequency range of AEM systems, which have a general sensitivity to τ ranging from 10^{-2} to 10^{-4} s (Macnae, 2016a, 2016b; Viezzoli et al., 2017). The lower boundary is due to a combination of the base frequency of the system and duration of the current turn-off ramp. In fact, it is during the current ramp-down that AEM systems charge up the ground, while creating the electromagnetic force causing charge separation. The slower the ramp, the lower the τ that can potentially be excited and measured. In order to illustrate this point we revert to individual forward responses. In Fig. 4 we compare responses from the relatively slow ramp-down (~1 ms) of a VTEM system versus the faster (~5 μs for low moment and ~50 μs for high moment) ramp-down of a SkyTEM system, for the same thickness of the top chargeable layer of Fig. 2. The shorter ramp of the SkyTEM system yields smaller responses associated with near-surface variations than for VTEM. Note that, in the absence of chargeability, the result would revert to the opposite situation, with which the AEM community is familiar, where SkyTEM is more sensitive to the near surface.

The augmented sensitivity of AEM to the near surface in the presence of chargeable material suggests a corresponding increase in dependency on the system's altitude. Fig. 5 confirms this.

The dB/dt($\mathbf{J}_{ip}$) introduces a very strong dependency on system altitude, which ends up also affecting the total dB/dt($\mathbf{J}_{tot}$), well beyond the dependency on altitude of the pure EM currents dB/dt($\mathbf{J}_{em}$). This

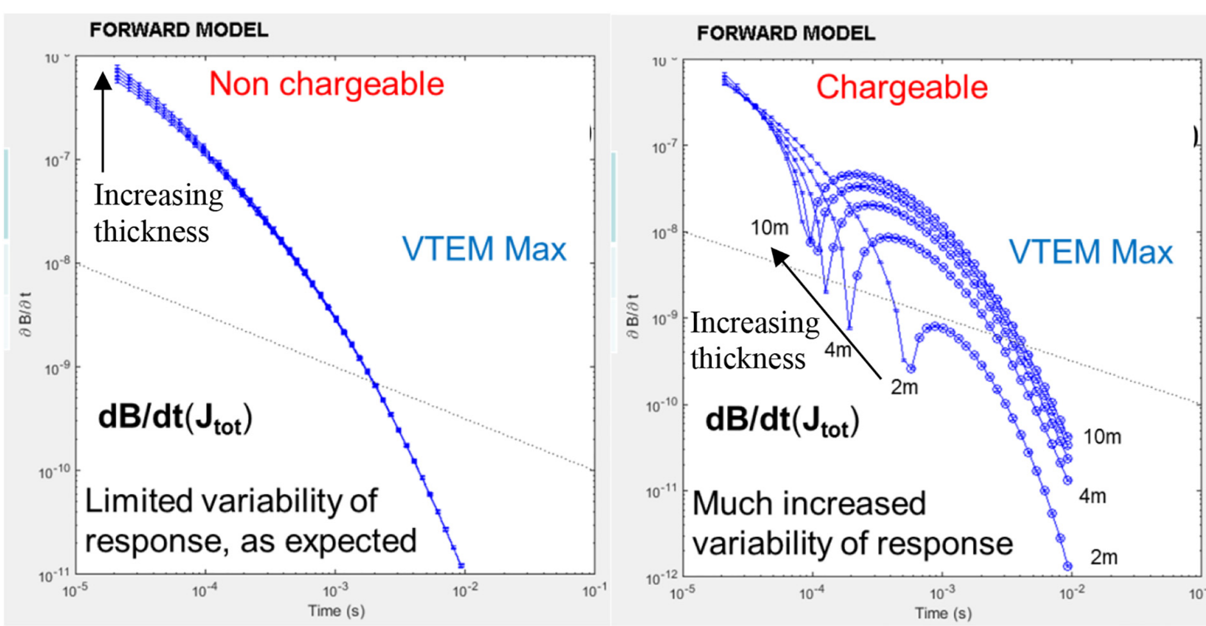

Fig. 2. Synthetic response of a VTEM-like system for a series of two-layer models showing the effect of chargeability on sensitivity to thickness of shallow chargeable layers. The bottom layer is always resistive (1000 Ωm) and non-chargeable; (left panel) non-chargeable top layer (200 Ωm), (right panel) chargeable top layer (300 mV/V, c = 0.7, τ = 1 ms) both of varying thickness (2 m to 10 m, at 2 m intervals).

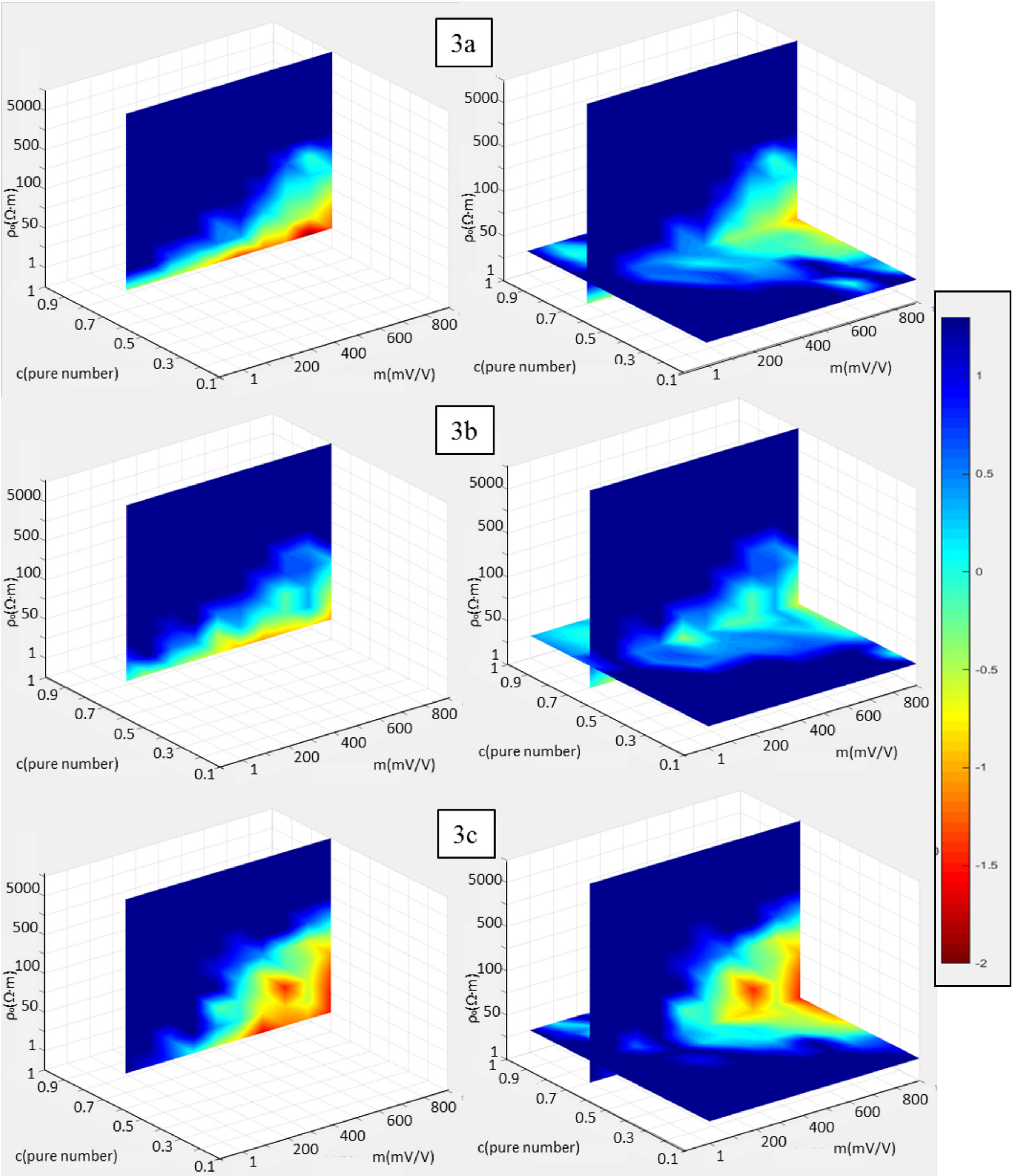

Fig. 3. Sensitivity (expressed as log10 (STDF-1), refer to text for more details) to *thickness* (top two panels), *resistivity* (central panels) and *chargeability* (bottom panels) of the top layer, for a series of two-layer models (cfr text for details), versus the first layer's Cole-Cole parameter variations (with τ fixed to 10^{-4} s). The top layer is 20 m thick, and the lower layer is resistive (1000 Ωm) and non-chargeable. Red colours represent parameters that are well resolved, and blue is poorly resolved. The right column shows the sensitivity cube cut by two planes (ρ and c constant), the right column by one (constant c). (For interpretation of the references to colour in this figure legend, the reader is referred to the web version of this article.)

implies that accurate measuring and recording of actual system altitudes becomes even more crucial than in the absence of IP (cf Christiansen et al., 2011). Thus far we have focussed on sensitivity to the near surface. However, the AIP trap will also create artefacts in the resistivity model below a surface chargeable layer, if the IP effect is overlooked or not modelled correctly. This is evident from Fig. 1.

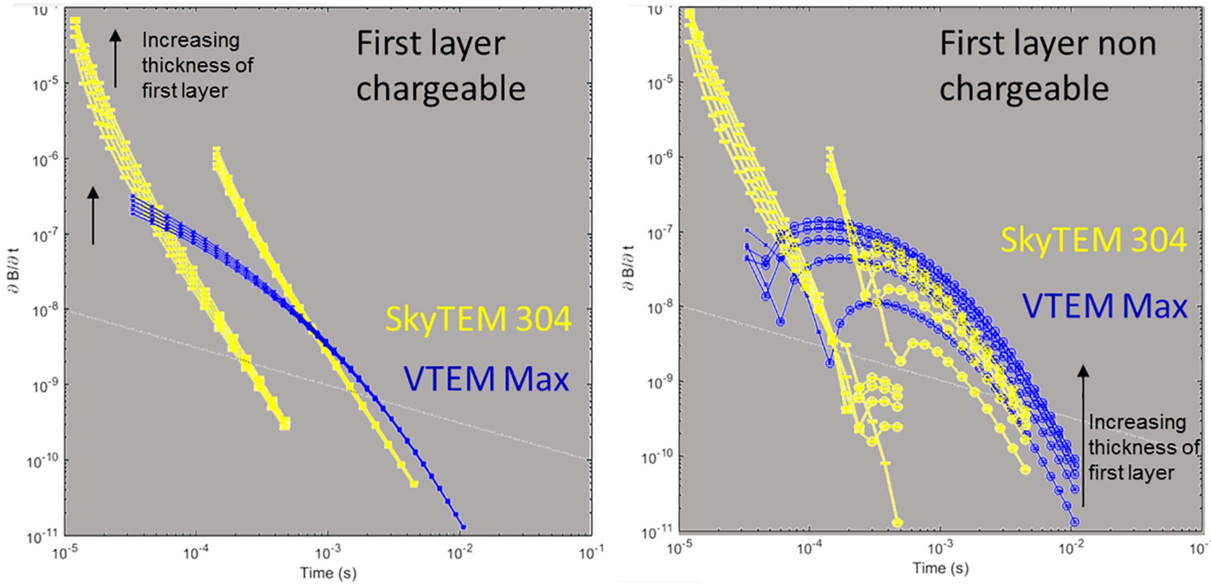

Fig. 4. Responses of VTEM and SkyTEM systems for a series of two-layer models, showing the effect of chargeability on sensitivity to thickness of shallow chargeable layers. The bottom layer is always resistive (1000 Ωm) and non-chargeable; (left panel) non-chargeable top layer (100 Ωm), (right panel) chargeable top layer (ρ = 100 Ωm, m = 300 mV/V, c = 0.7, τ = 1 ms), both of varying thickness (2 m to 10 m, at 2 m intervals). The dashed grey line shows a typical noise level.

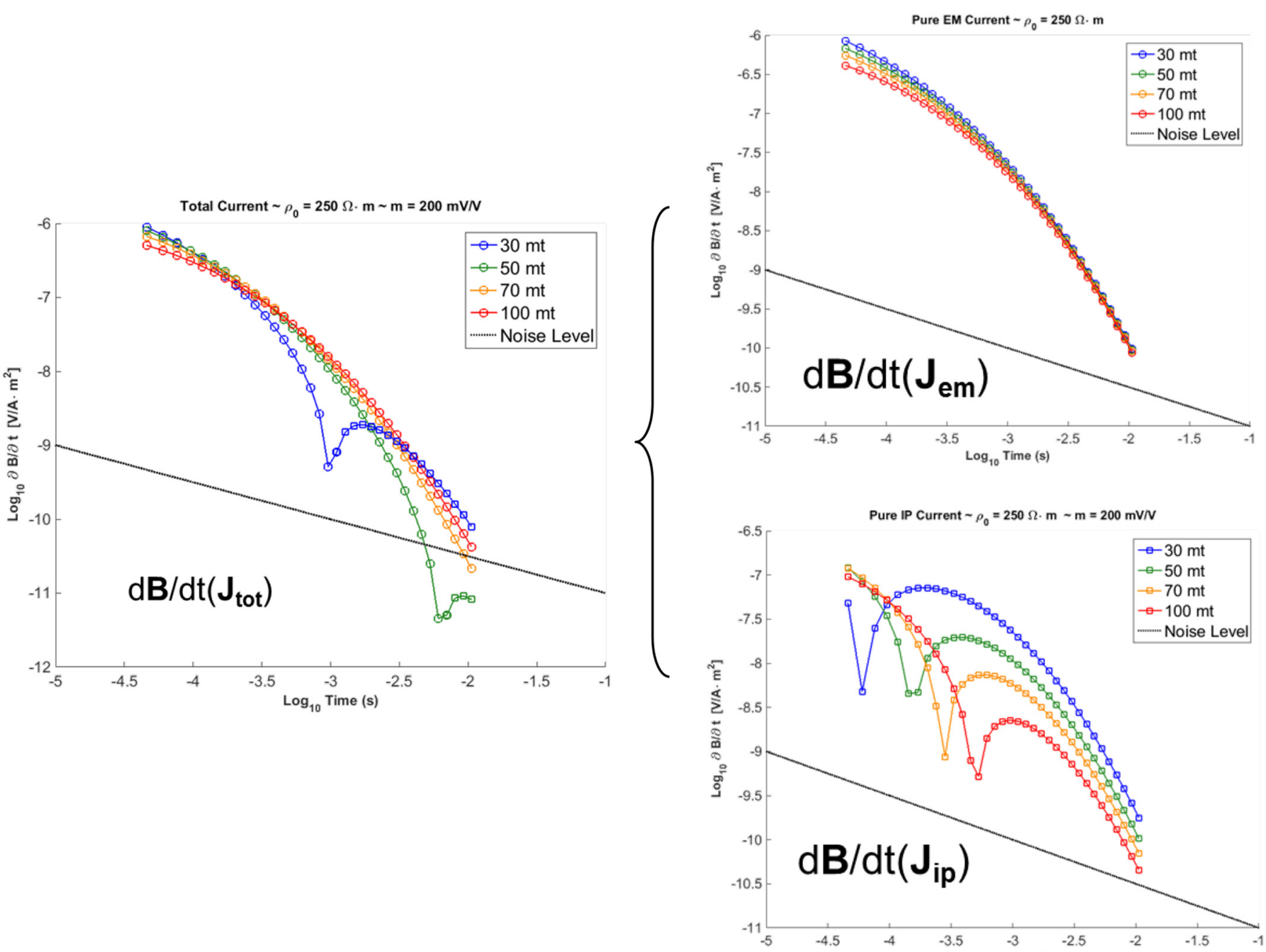

Fig. 5. Effect of AEM system altitude on measured responses in the presence of a chargeable top layer (200 mV/V, 250 Ωm, c = 0.5, τ = 10^{-3} s, 20 m thick) and resistive (1000 Ωm), non-chargeable basement.

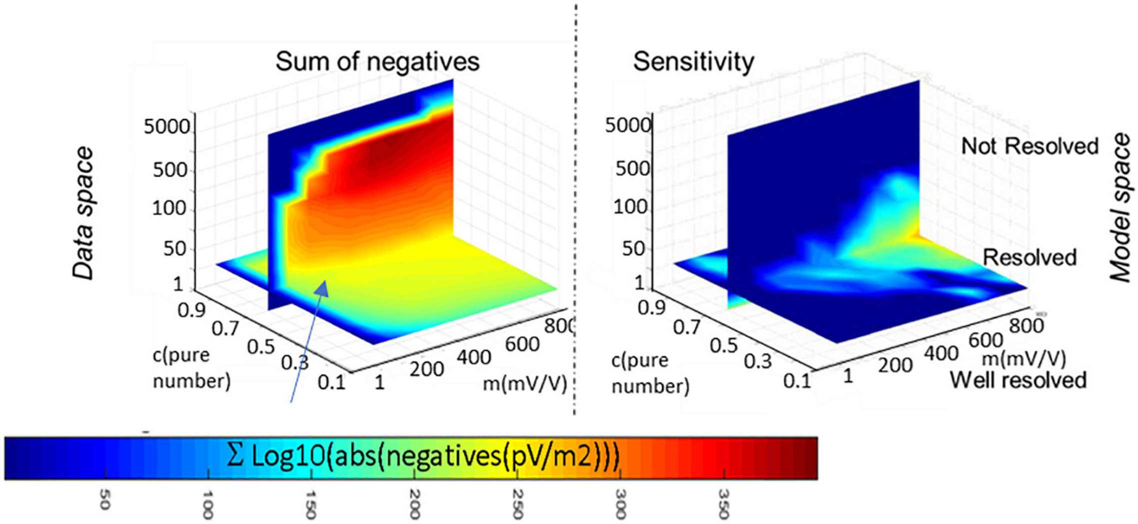

Fig. 6. Correlation between AIP signatures in data space (left) versus sensitivity in model space (right, same colorscale as Fig. 3).

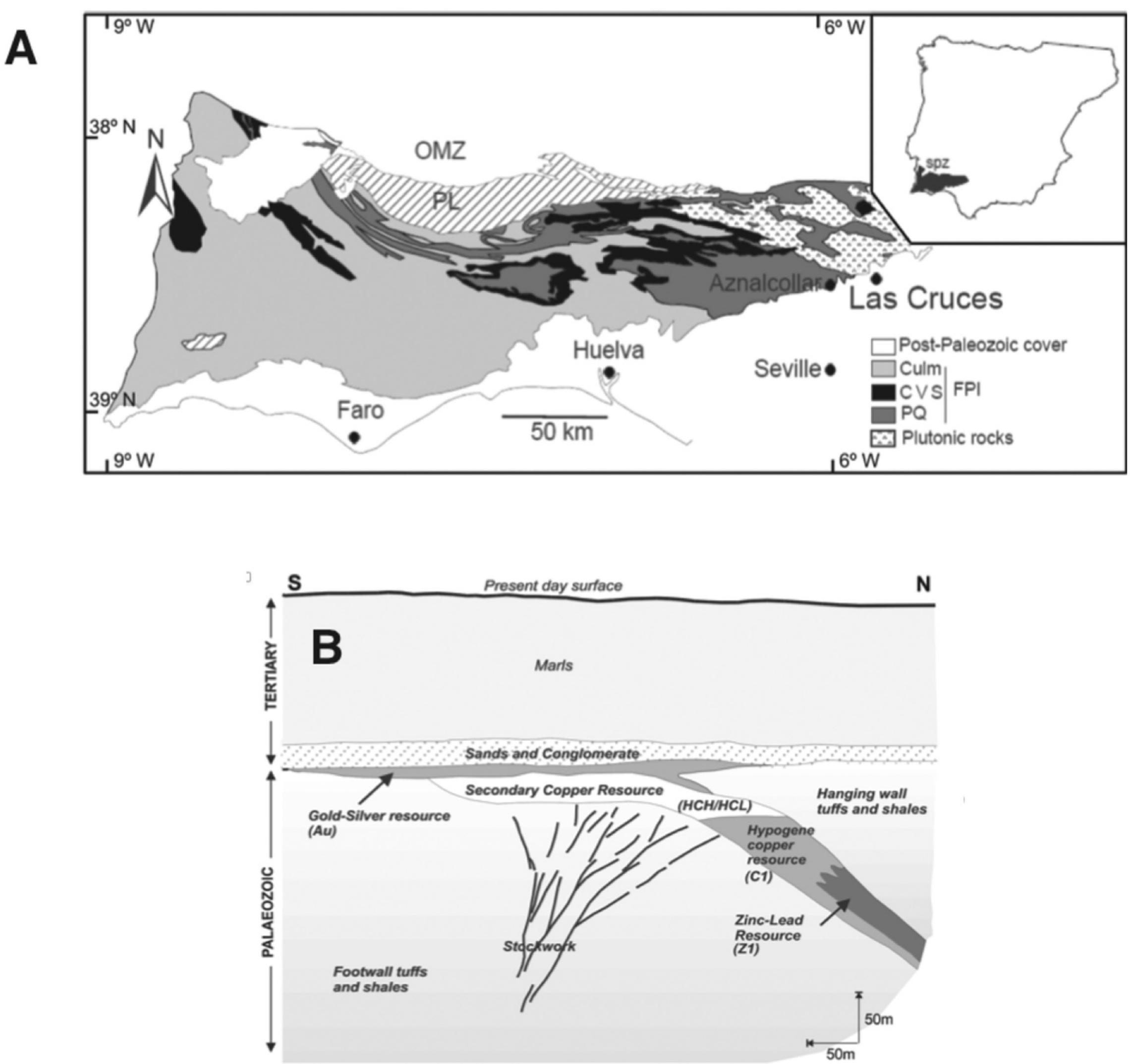

Fig. 7. (a) Las Cruces regional geological setting in the Iberian Pyrite Belt (after Yesares et al., 2015) showing the limit of outcropping volcanic host rocks just north of Las Cruces. The very conductive post-Paleozoic cover, averaging less than 5 Ωm in the Las Cruces area, deepens steadily towards the south from its northern limit. (b) Las Cruces schematic geologic cross section (after McIntosh et al., 1999) illustrating the conductive marl cover over the deposit. HCH/HCL indicates the chalcocite enrichment blanket, and the hypogene sulphide orebody dips at ~45 degrees northward.

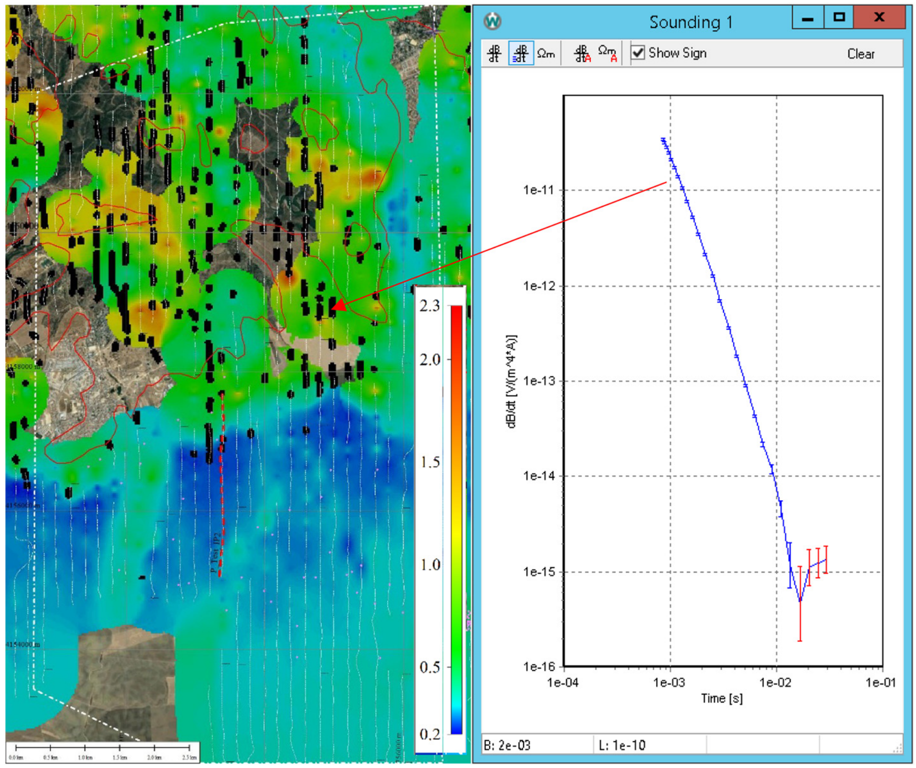

Fig. 8. (left) Map of the AEM decay constant at late times for the area subsequently modelled with AIP.The solid red line indicates the northern limit of cover, including isolated patches north of that. The entirety of the cover is very conductive (~0.2 S/m) and, in the absence of IP effects, is expected to have a uniformly large decay constant. Low values of the decay constant are therefore associated with greater IP effects in the data. Negative time gates (above noise level) in the SkyTEM transients are indicated in black The red dotted line traces the location of the cross sections shown in Figs. 9 and 10. (right) Example of a transient affected by IP (negative voltages in red).

Modelling the actual measured signal dB/dt($\mathbf{J}_{tot}$) as if it were just dB/dt ($\mathbf{J}_{em}$), would result in erroneous resistivity models, even if all negative values in dB/dt($\mathbf{J}_{tot}$) decays are culled, which has been the original practice in the AEM community to mitigate IP effects.

The potential effect of an increase in near-surface sensitivity of AEM systems associated with shallow chargeable material should not be ignored. The presence of overburden giving a measureable AIP effect has been widely reported (e.g., Macnae, 2016a, 2016b) at different latitudes and for different geologic materials (e.g., Arctic permafrost and Australian weathered regolith). Complicating the study of these IP sources, the IP phenomenon occurring at the frequency range typical of AEM systems (25 Hz) may have different origins to those measured by ground IP systems typically operating at 0.125 Hz. Furthermore, the common wisdom that unbiased very early times (or conversely high frequencies) are a general prerequisite to resolve shallow layers of limited conductance is, to a degree, challenged. When AIP traps the measured signal in the near surface, AEM systems with limited high frequencies can resolve this. Other implications include an increase in the sensitivity to the ground clearance of the transmitter/receiver frame, with the associated need to better monitor system altitude. As discussed, the AIP trap will also result in erroneous resistivity models at depths below any surface chargeable material, should the IP effects be ignored or not modelled properly.

The modelling conclusions of this study remain valid, at least qualitatively, for any alternative IP model (e.g, Debye), and/or for other helicopter TDEM systems with different specifications. It is also valid for IP effects in ground (central loop) TDEM, with the only exception being the dependency on flying height.

The relationship between data space (the measured signal) and model space (the Cole-Cole parameters) in the presence of AIP becomes complicated. While an attempt to derive a full description of AIP effects in the data space is attractive, it is risky because the data-to-model space mapping with AIP is too complex, and somewhat "unpredictable", when compared to pure EM. This is illustrated in Fig. 6, which reports further analysis on the correlation between data (left, sum of negatives) and model space (right, sensitivity to thickness of first layer, cfr Fig. 3 and relative text for more details).

The improvement in near-surface sensitivity in model space does not necessarily coincide with the areas of strongest measurable IP effects in the data space (i.e., sum of negative voltages, with negatives being the only unequivocal indication of IP effects). The same holds true for the correlation between negatives and other Cole-Cole parameters (e.g., m). The consequence is that a full robust assessment of the AIP effects in a given AEM survey demands full modelling (inversion) of at least a subset of the survey.

2.1. Depth of cover mapping at Cobre Las Cruces, Spain

A 12.5 Hz SkyTEM dataset was acquired in 2017 by First Quantum Minerals Ltd. around the Las Cruces mine in Andalucia, southern Spain. Las Cruces is a volcanogenic massive sulphide (VMS) deposit in the Iberian Pyrite Belt, hosted in a volcano-sedimentary series sitting under more than 100 m of post-mineral, conductive marl cover (Fig. 7). A horizontal chalcocite zone overlies a fresh sulphide zone dipping at about 45 degrees towards the north. A sulphide stockwork of lower grade and barren rock sits below the chalcocite enrichment zone. One of the challenges to further exploration is accurate mapping of the base of thick conductive cover (<10Ωm), which was the main goal of the AEM survey.

The data and inversion results show some obvious IP effects manifesting as negative transients (e.g., Fig. 8) and areas of high misfit not due to 3D effects. Comparison with drilling suggests that ignoring IP by deleting negative transients results in some artefacts in the AEM-derived resistivity and depth to basement, when the latter is in the 0 to 100 m range. Cobre Las Cruces is one of the reference sites in an EU Horizon 2020 project called INFACT. One of the innovative technology components of INFACT is the robust modelling of IP effects, and the

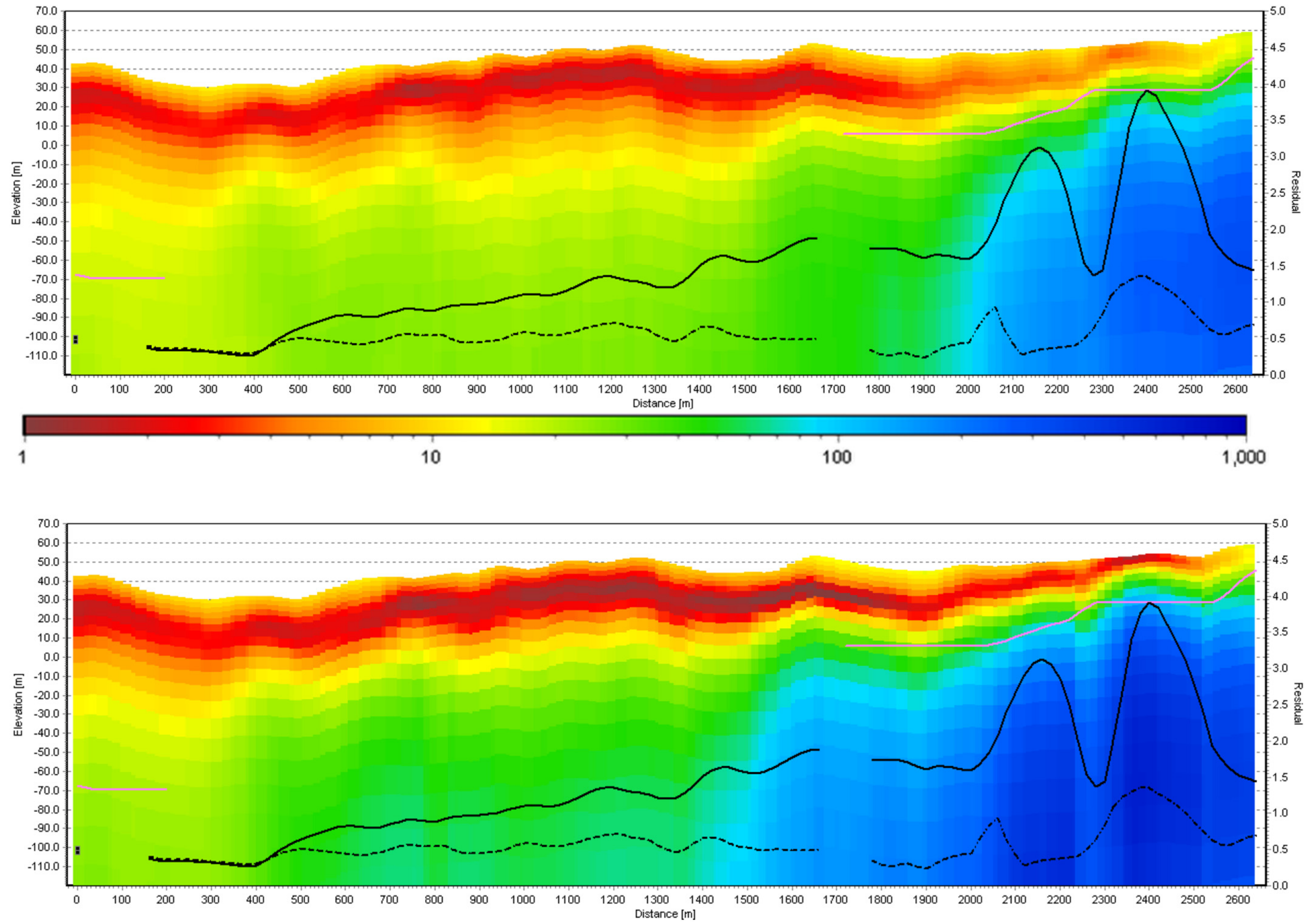

Fig. 9. Cross sections comparing resistivity (Ωm) resulting from standard modelling ignoring IP (bottom) and AIP modelling (top panel) against drilling information. The pink line traces the depth of cover from drillholes close to the profile. When IP is modelled, the depth of conductive cover is deeper and more closely matches the drilled depth of cover. The dashed black line shows the misfit when AIP is modelled, and the solid black line demonstrates the much larger misfit without AIP modelling. The near-surface conductivity is amplified in the top panel when the AIP contribution is ignored. (For interpretation of the references to colour in this figure legend, the reader is referred to the web version of this article.)

12.5 Hz SkyTEM data at Las Cruces provide a good case study to assess the benefits of modelling IP. The conductive and chargeable post-mineral cover deepens gradually from north to south over resistive volcanic bedrock, providing an ideal geologic situation for 1D modelling free of interfering 3D effects.

A portion of the dataset was processed twice, once assuming purely inductive EM and once to retain all IP effects in the data. With the objective of comparing the accuracy in mapping depth of cover with reference to drillhole logs, the subset in Fig. 8 was chosen to coincide with good drilling control in an area identified with probable IP effects. The majority of drill holes are located in areas that display a limited number of negative transients, but uniformly fast decays.

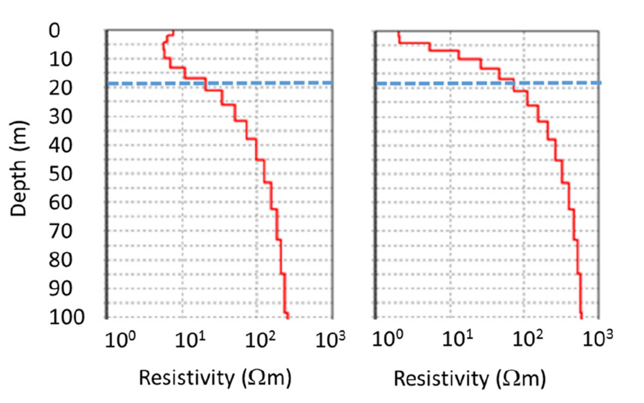

Fig. 10. 1D resistivity models at distance = 2275 m in section above with (left) and without (right) IP modelling, compared against interpolated depth to basement from drilling (dashed blue line) at same location. (For interpretation of the references to colour in this figure legend, the reader is referred to the web version of this article.)

The reprocessed data was inverted with AarhusInv, which allows Cole-Cole parameters to be modelled. Fig. 9 compares the results with and without IP modelling against the depth to bedrock according to drillholes. When IP is not modelled the negatives are deleted and we only solve for ρ. When modelling IP, negatives are retained and we solve for r, m, c and τ (the latter two with tight spatial constraints cfr Viezzoli et al. 2016 for details). The regularization on the resistivity models is the same in both cases. When AIP is modelled, the transition between conductive cover and resistive basement is a better match to the depth of cover logged in drill holes (Figs. 9 and 10). Where drilled depth to basement ranges between 0 and ~50 m, overlooking IP causes a) an underestimation of this depth, b) an exaggeration of lateral variations in depth, and c) an increase in data misfit. When the conductive cover is very deep (left-hand side of Fig. 9), the inclusion of IP modelling ceases to have an effect on the results because the overall conductance of the cover layer overwhelms the IP effect.

Fig. 11 shows the chargeability section extracted from the AEM data. Processing can recover chargeability m for cover <50 m, and the bottom of the chargeable anomaly matches the depth to bedrock from drilling. Despite no documented lateral variability in the composition of the

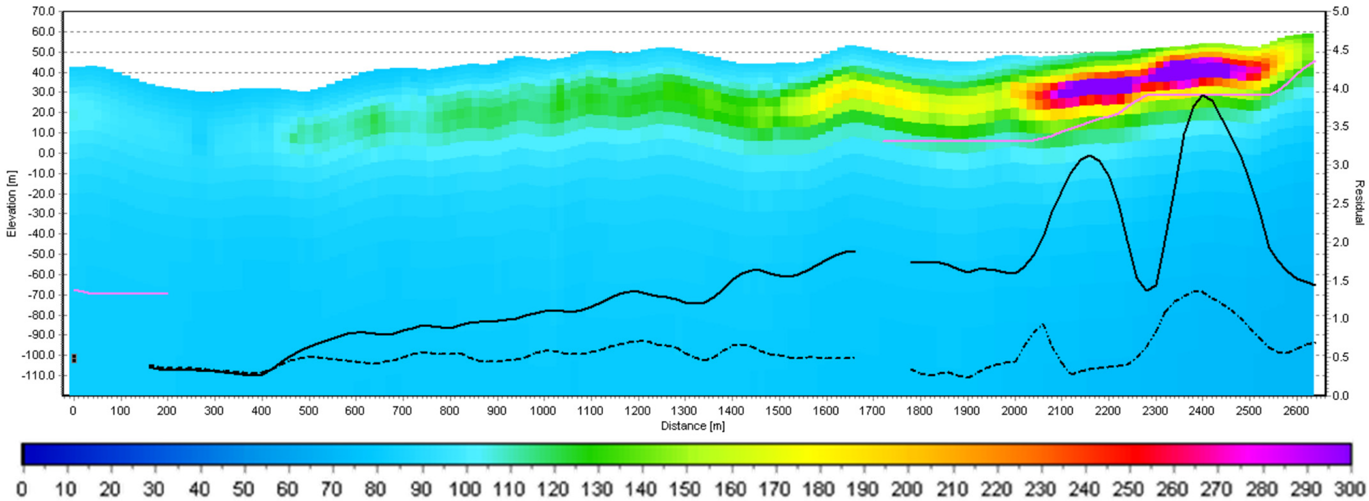

Fig. 11. Cross section from Fig. 9 comparing chargeability (mV/V) resulting from AIP modelling, against drilling information. The pink line traces the depth of cover from drillholes close to the profile.The dashed and solid black lines show the misfit with and withoutAIP modelling, respectively. (For interpretation of the references to colour in this figure legend, the reader is referred to the web version of this article.)

cover, when the cover becomes thicker, its EM conductance masks possible AIP effects and the sensitivity to m becomes too low for it to be recovered.

The modelled depth of cover from the EM is compared more quantitatively to 40 drillholes in the area in Fig. 12. Resistivity values are read from the inverted EM sections at the depths where base of cover is logged in drill holes. That is, the drillhole base of cover is used to determine the associated resistivity value at this interface. The frequency histogram of this resistivity distribution is shown in Fig. 12 for the cases of modelling with and without AIP effects, for the whole survey. In the first case the average value is 13 Ωm, in the second it is 20 Ωm. The distribution of resistivity values associated with base of cover is much tighter when AIP effects are included in the modelling. The implication is that if AIP effects are ignored, an attempt to predict depth to basement using isoresistivity surfaces derived from automatic picking of specific resistivity values would result in larger errors. This is due to the physics of AIP effects discussed above. Refer to Fig. 1: the positive part of a measured transient is distorted (decays faster than with pure EM) in a way that can be fitted by a non-dispersive model with erroneously low conductivity and thickness of the first layer, and excessively high resistivity of the second layer (cf also Viezzoli et al., 2017). As the conductive and chargeable layer becomes so thick that the pure EM response renders the IP currents negligible, these artefacts will decrease. The consequences for prediction of resistive basement based on a single resistivity

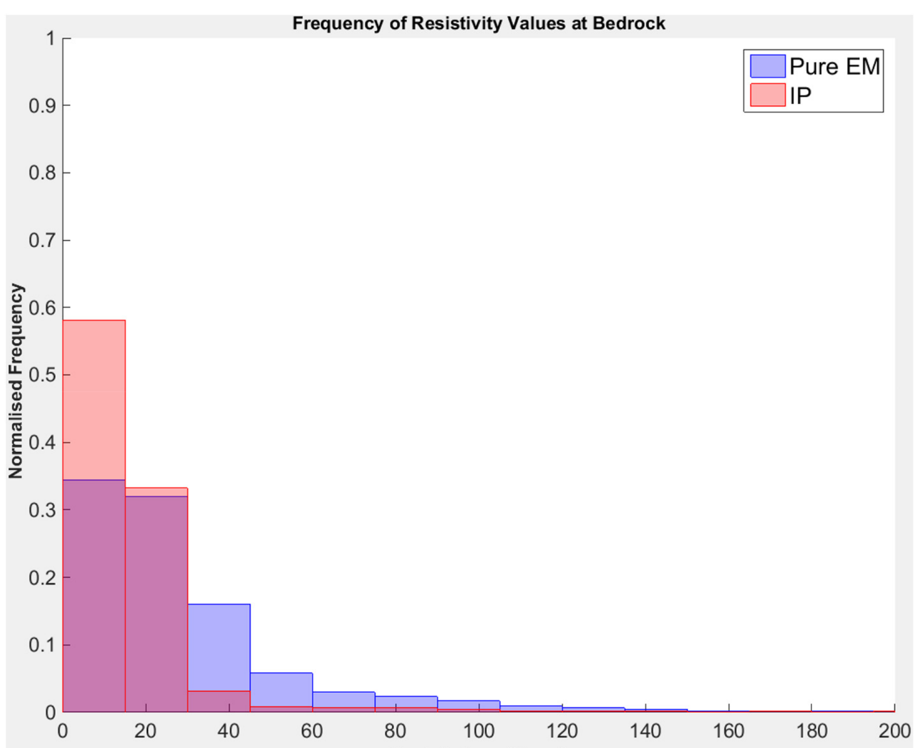

Fig. 12. Frequency histogram of the inverted EM resistivity values at the logged depths of base of cover on drill holes. The comparison for modelling with AIP and without AIP (pure EM). It shows that the distribution is much tighter when AIP effects are accounted for.

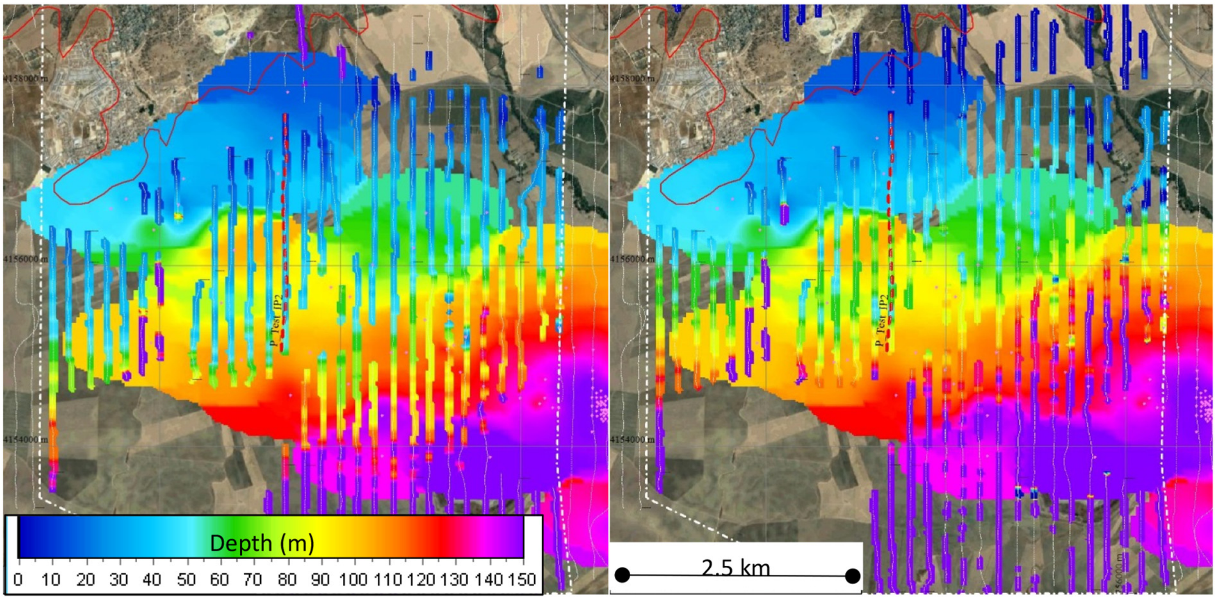

Fig. 13. Depth to basement interpolated from drilling (continuous background) versus depth to resistive basement as predicted from inversion of SkyTEM data shown as coloured strips along flight lines, without modelling AIP (left) and with AIP modelled (right). Each comparison uses the best average match between drillhole control and inverted resisitivty, which is 20 Ωm without AIP and 13 Ωm when AIP is modelled.The match is visually more similar when AIP effects are included.

value is that any isoresistivity depth surface would have exaggerated lateral variations, being either underestimated in shallower cover or overestimated in thicker cover. Note that this holds true regardless of the actual resistivity value (with associated resistivity) adopted to predict the depth to basement, implying that any attempt to "recalibrate" the AEM resistivity models with ancillary data, whilst fitting the AEM data, is bound to fail.

In order to illustrate this effect, two isoresistivity surfaces predicting depth to basement were derived, one with, and the other without IP modelling. In the AIP case, the predicted depth to basement is associated with the resistivity threshold of 13 Ωm (lower resistivity in the cover above, higher resistivity in the bedrock below); in the non AIP case it was associated with 20 Ωm. Fig. 13 compares absolute values of bedrock depth estimates with actual drilled bedrock depth. AIP modelling yields better visual correlation with drilling.

The error in prediction estimate (i.e., 100 x abs((predicted-true)/true)) is calculated in Fig. 14. Modelling IP generally decreases the errors in prediction significantly, halving it over large areas. It also produces a much more stationary field of percent error with respect to non IP modelling, which, for the reasons discussed above, displays much higher lateral gradients. This SkyTEM survey, with a 12.5 Hz base frequency, high moment, relatively late first gate (~130 μs), and slow ramp down was not intended for near-surface mapping. Despite this, the prediction error for shallow (~20 m) cover thickness with IP is on

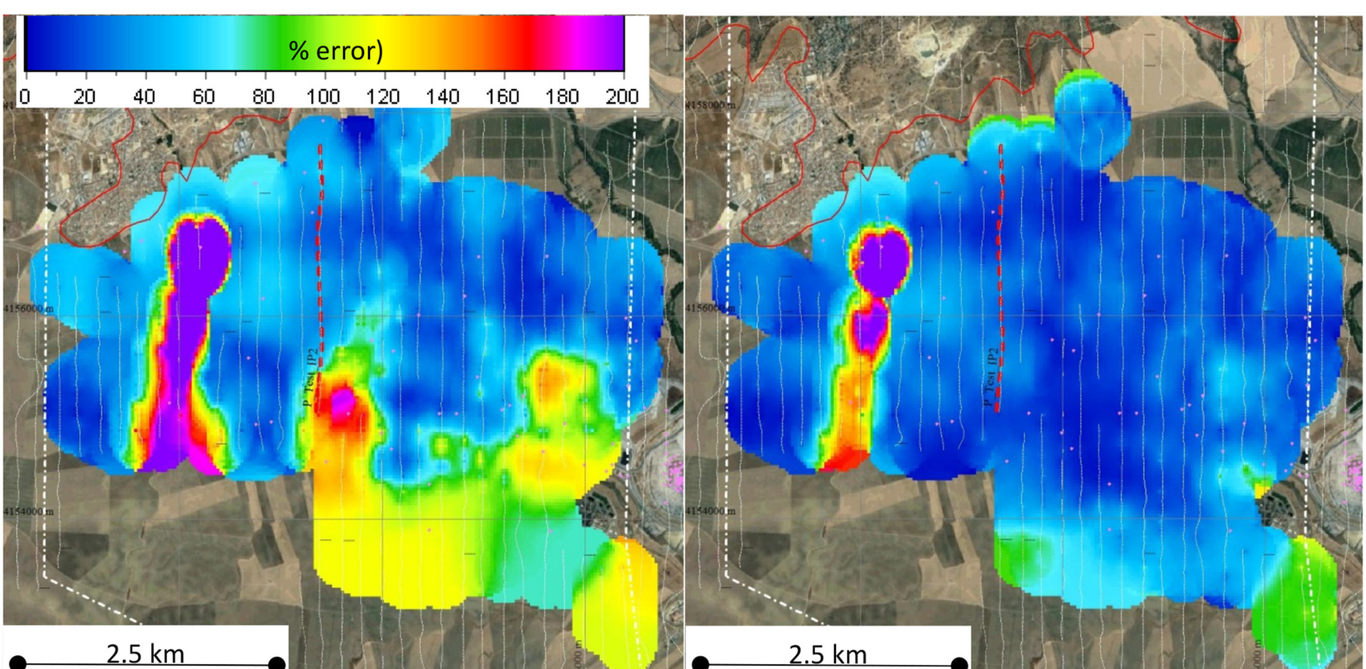

Fig. 14. Error (%) in prediction of depth to basement from inversion of SkyTEM data without (left) and with (right) AIP modelling, compared against drilling information.

the order of 20%. In the total absence of chargeability in the cover it would have been worse, as discussed above and described in Fig. 3a. The results prove that customized AIP processing and modelling improves the prediction accuracy of depth to resistive basement from AEM data affected by IP.

Complementary VTEM data with different waveforms will be acquired at Las Cruces during the INFACT research project to further study the effect of system specification on AIP.

3. Conclusions

Numerical modelling illustrates the physics associated with dispersive mechanisms in electrical resistivity, and the effects on interpretation of inverted EM data. The entire TDEM transient recorded by a central loop EM system can be confined to the near-surface by the presence of chargeable material there, a phenomenon we call the "AIP trap". The consequence for airborne surveys is a potentially significant increase in the sensitivity of helicopter central loop TDEM systems to near-surface resistivity and thickness. Sensitivity to system altitude also increases markedly. A case study involving conductive and chargeable cover over resistive basement in southern Spain confirms that modelling AIP improves the accuracy when predicting depth to resistive basement, while failure to model IP effects leads to more artefacts and excessive lateral variability in the prediction. As near- surface conductance increases, via deepening cover in the Spanish case study, the pure EM contribution to the transients increases and eventually masks any IP effects. The implications of this study for shallow, near-surface chargeable layers are relevant for geotechnical and environmental applications as well as depth of cover mapping.

Authors declaration

Anyway, I hereby certify that the work presented herein is the product of research carried out by the authors.

Declaration of Competing Interest

The authors declare that they have no known competing financial interests or personal relationships that could have appeared to influence the work reported in this paper

Acknowledgements

This project has received funding from the European Union's Horizon 2020 research and innovation programme under grant agreement No 776487.

References

Auken, E., Christiansen, A.V., 2004. Layered and laterally constrained 2D inversion of resistivity data. Geophysics 69, 3,752–761.

Christiansen, A.V., Auken, E., Viezzoli, A., 2011. Quantification of modeling errors in airborne TEM caused by inaccurate system description. Geophysics 76 (1), F43–F52.

Fiandaca, G., Auken, E., Christiansen, A.V., Gazoty, A., 2012. Time-domain-induced polarization: Full-decay forward modeling and 1D laterally constrained inversion of Cole-Cole parameters. Geophysics 77, E213–E225 no. 3.

Kang, S., Fournier, D., Oldenburg, D.W., 2017. Inversion of airborne geophysics over the DO-27/DO-18 kimberlites - part 3: Induced polarization. Interpretation 5, T327–T340.

Macnae, J., 2016a. Quantitative estimation of intrinsic induced polarization and superparamagnetic parameters from airborne electromagnetic data. Geophysics E433–E446.

Macnae, J., 2016b. Comparing induced polarization responses from airborne inductive and galvanic ground systems: Tasmania In. Geophysics 81, E471–E479.

McIntosh, S.M., Gill, J.P., Mountford, A.J., 1999. The geophysical response of the Las Cruces massive sulphide deposit. Explor. Geophys. 30, 123–134.

Nabighian, M.N., 1979. Quasi-static transient response of a conducting half-space; an approximate representation. Geophysics 44 (10), 1700–1705.

Smith, R.S., 1989. Discussion on: "Induced polarization effects in time domain electromagnetic measurements". Geophysics 54, 514–523.

Viezzoli, A., Manca, G., 2019. On airborne IP effects in standard AEM systems: tightening model space with data space. Explor. Geophys. https://doi.org/10.1080/08123985.2019.1681895.

Viezzoli, Kaminski, Fiandaca, 2017. Modeling induced polarization effects in helicopter TEM data: Synthetic case studies. Geophysics 82–2, 1–20.

Yesares, L., Sáez, R., Nieto, J., Almodóvar, G., Gómez, C., Escobar, J., 2015. The Las Cruces deposit, Iberian Pyrite Belt, Spain. Ore Geol. Rev. 66, 25–46. https://doi.org/10.1016/j.oregeorev.2014.10.019.